Tumor Biol. (2016) 37:2365–2378
DOI 10.1007/s13277-015-4015-9

ORIGINAL ARTICLE

A molecular and biophysical comparison of macromolecular changes in imatinib-sensitive and imatinib-resistant K562 cells exposed to ponatinib

Melis Kartal Yandim[1] · **Cagatay Ceylan**[2] · **Efe Elmas**[2] · **Yusuf Baran**[1,3]

Received: 1 August 2015 / Accepted: 28 August 2015 / Published online: 15 September 2015

Abstract Chronic myeloid leukemia (CML) is a type of hematological malignancy that is characterized by the generation of Philadelphia chromosome encoding BCR/ABL oncoprotein. Tyrosine kinase inhibitors (TKIs), imatinib, nilotinib, and dasatinib, are used for the frontline therapy of CML. Development of resistance against these TKIs in the patients bearing T315I mutation is a major obstacle in CML therapy. Ponatinib, the third-generation TKI, is novel drug that is effective even in CML patients with T315I mutation. The exact mechanism of ponatinib in CML has been still unknown. In this study, we aimed to determine the potential mechanisms and structural metabolic changes activated by ponatinib treatment in imatinib-sensitive K562 human CML cell lines and 3 μM-imatinib-resistant K562/IMA3 CML cell lines generated at our lab. Apoptotic and antiproliferative effects of ponatinib on imatinib-sensitive and 3 μM-imatinib-resistant K562/IMA3 CML cells were determined by proliferation and apoptosis assays. Additionally, the effects of ponatinib on macromolecules and lipid profiles were also analyzed using Fourier transform infrared spectroscopy (FTIR). Our results revealed that ponatinib inhibited cell proliferation and induced apoptosis as determined by loss of mitochondrial membrane potential, increased caspase-3 enzyme activity, and transfer of phosphatidylserine to the plasma membrane in both K562 and K562/IMA-3 cells. Furthermore, cell cycle analyses revealed that ponatinib arrested K562 and K562/IMA-3 cells at G1 phase. Moreover, ponatinib treatment created a more ordered nucleic acid structure in the resistant cells. Although the lipid to protein ratio increased in imatinib-sensitive K562 cells with a little decrease in the K562/IMA-3 cells, ponatinib treatment indicated significant changes in the lipid composition such as a significant increase in the cellular cholesterol amounts much more in the K562/IMA-3 cells than the sensitive counterparts. Unsaturation in lipids was higher in the resistant cells; however, increases in lipids without phosphate and the number of acyl chains were much higher in the K562 cells. Taken together, all these results showed powerful antiproliferative and apoptotic effects of ponatinib in both imatinib-sensitive and imatinib-resistant CML cells in a dose-dependent manner, and hence, the use of ponatinib for the treatment of TKI-resistant CML patients may be an effective treatment approach in the clinic. More importantly, these results showed that FTIR spectroscopy can detect drug-induced physiological changes in cancer drug resistance.

Keywords Ponatinib · Chronic myeloid leukemia (CML) · Multidrug resistance (MDR) · Imatinib · Fourier transform infrared spectroscopy (FTIR)

✉ Cagatay Ceylan
cagatayceylan@iyte.edu.tr

✉ Yusuf Baran
ybaran@gmail.com

[1] Department of Molecular Biology and Genetics, İzmir Institute of Technology, Urla 35430, İzmir, Turkey

[2] Department of Food Engineering, İzmir Institute of Technology, Urla 35430, İzmir, Turkey

[3] Department of Molecular Biology and Genetics, Faculty of Life and Natural Sciences, Abdullah Gul University, Kayseri, Turkey

Introduction

Chronic myeloid leukemia (CML), a type of hematological malignancy, is characterized by the reciprocal translocation between the breakpoint cluster region (BCR) gene on chromosome 22 and the Abelson murine leukemia virus (ABL) gene on chromosome 9, t(9;22)(q34;q11). This translocation

results in the formation of Philadelphia (Ph) chromosome coding for BCR/ABL fusion protein having constitutively active tyrosine kinase activity [1]. BCR/ABL can phosphorylate and activate many signaling molecules inducing cell proliferation and survival. For this reason, tyrosine kinase inhibitors (TKIs) are the main drugs used in CML therapy [2]. In the clinic, tyrosine kinase inhibitors are used as frontline therapy due to their efficiency in acquiring early optimum responses in CML [3]. However, resistance can be observed in many cases via several ways [4]. T315I mutation, one of the frequently encountered mutations, causes an important obstacle in CML therapy. This mutation results in the switch of the amino acid threonine at position 315 into isoleucine [5]. Patients bearing T315I mutation are resistant to imatinib, nilotinib, and dasatinib [6].

The third-generation TKI, ponatinib, is an FDA-approved drug that is effective even in CML patients with T315I mutation [7]. This isoleucine residue removes the hydrogen bond and prevents the TKIs to bind to the ATP-binding pocket of BCR/ABL. Since ponatinib bears a particular carbon–carbon triple bond preventing the steric hindrance as a result of T315I mutation, it can bind and inhibit BCR/ABL kinase. In addition to BCR/ABL kinase, ponatinib can also inhibit Src kinase, KIT, FLT3, PDGFR, VEGFR, and FGFR [8].

Fourier transform infrared spectroscopy allows for rapid, sensitive, and non-destructive method analysis of samples in any physical state [9, 10]. It monitors molecular changes in the analysis of biological systems at the functional group level. The digital spectral data can be analyzed with many different manipulations. These manipulations yield both qualitative and quantitative information. In obtaining spectral data, shifts in peak positions and changes in bandwidths and band intensities are used to obtain structural and functional information and also changes in cellular components such as lipids, proteins, carbohydrates, and nucleic acids in the systems analyzed [9, 11]. The changes in the studied tissue or cells indicate specific biological differentiation processes such as disease progression.

In this study, we aimed to examine apoptotic and antiproliferative effects of ponatinib, and also its effects on macromolecules and lipid profiles in imatinib-sensitive and imatinib-resistant K562/IMA-3 CML cells. For this purpose, imatinib resistance was induced in K562 cells. Although resistance-dependent macromolecular changes in various types of cancers against different anticancer drugs including nilotinib have been investigated using Fourier transform infrared spectroscopy (FTIR) technique [12–14], this is the first detailed study investigating the changes between imatinib-sensitive and imatinib-resistant K562/IMA-3 cells in terms of biochemical variations.

Materials and methods

Cell lines and chemicals K562 human chronic myeloid leukemia cells were obtained from German Collection of Microorganisms and Cell Cultures (Germany). Ponatinib was obtained from Selleck Chem Chemicals (USA), and stock solution (162 mM) was dissolved in dimethylsulfoxide (DMSO). Imatinib mesylate was obtained from Novartis (Gleevec, USA).

Culture conditions K562 and K562/IMA-3 human chronic myeloid leukemia cells were maintained in RPMI-1640 growth medium containing 10 % fetal bovine serum and 1 % penicillin–streptomycin (Invitrogen, Paisley, UK) at 37 °C in 5 % CO_2. K562/IMA-3 cells were generated in our lab.

Measurement of cell proliferation by MTT assay Cytotoxic effects and IC_{50} values (drug concentrations inhibiting cell proliferation by 50 %) of ponatinib on K562 and K562/IMA-3 cells were determined by MTT cell proliferation assay as explained [15].

Examining the loss of mitochondrial membrane potential Apoptotic effects of ponatinib on K562 and K562/IMA-3 CML cells were examined by using a JC-1 mitochondrial membrane potential detection kit (Cell Technology, USA) as explained [16]. This kit uses JC-1, a unique cationic dye, to signal the loss of the MMP. JC-1 accumulates in the mitochondria and stains red in non-apoptotic cells while JC-1 remains in the cytoplasm as a monomer that stains green under fluorescent light in apoptotic cells.

Examining the changes in caspase-3 enzyme activity Changes in caspase-3 enzyme activity of the cells were examined by caspase-3 colorimetric assay kit (BioVision Research Products, USA). This assay is based on the spectrophotometric detection of the chromophore *p*-nitroanilide (*p*NA) after cleavage from the labeled substrate DEVD-*p*NA that can be recognized by caspases as explained [16].

Examining the apoptotic cell population by annexin-V FITC staining In order to confirm the results of caspase-3 enzyme activity and mitochondrial membrane potential analyses, we also determined the translocation of phosphatidylserine from the inner membrane to the outer cell membrane by using an annexin-V FITC staining kit (BioVision Research Products, CA) as explained [17].

Cell cycle analysis Effects of ponatinib on cell cycle were also assessed by cell cycle analysis in K562 and K562/IMA-3 CML cells. Cell cycle analysis is based on the determination of amounts of dsDNA by using propidium iodide, a DNA-

binding dye, via flow cytometry. When the data acquired from the flow cytometry are analyzed, cell cycle phases and the amounts of fragmented DNA of the cells can be determined as explained [16].

Sample preparation for FTIR spectroscopy In order to prepare the cells for FTIR spectroscopy, 5×10^6 cells were seeded into 75 cm^2 culture flasks with 20 ml of growth medium, and the cells were treated with IC_{50} values of ponatinib for each cell line (1.72 nM for K562 cells and 28.5 nM for K562/IMA-3 cells) for 72 h. After the incubation period, the cells were collected by centrifugation at 800 rpm for 5 min. Supernatants were removed, and the pellets were homogenized with PBS to be 5×10^6 cells/ml. The collected cells were lyophilized in a freeze drier (Labconco, FreeZone 18-l freeze dry system) overnight to remove water. The cell powder was mixed with dried potassium bromide (KBr) (Sigma-Aldrich, USA) in a mortar (at a ratio of 1:100). The mixture was then pressurized to 100 kg/cm^2 (1200 psi) for 5 min. All the cell growth, cell collection, and FTIR experiment for the imatinib-sensitive and imatinib-resistant K562 cells were carried out on the same day.

Lipid extraction In order to extract lipids from the cells, 10×10^6 cells were seeded into 75 cm^2 culture flasks with 20 ml of growth medium, and the cells were treated with IC_{50} values of ponatinib for each cell line (1.72 nM for K562 cells and 28.5 nM for K562/IMA-3 cells) for 72 h. After the incubation period, the cells were collected by centrifugation at 800 rpm for 5 min. Supernatants were removed, and the pellets were homogenized with PBS and then again centrifuged at 800 rpm for 5 min. Afterwards, the supernatant was removed and the cell pellet was homogenized with 2 ml of extraction mixture including chloroform/methanol (2:1, *v*/*v*) via vortexing. Then, the mixture was incubated for 20 min at room temperature. After the incubation period, 500 μl 37 % HCl was added onto the mixture, and after vortexing to homogenize the mixture, it was centrifuged at 500×*g* for 10 min. At the end of the centrifugation, the lower layer including chloroform was collected for the analysis [18].

FTIR spectrum accumulation and data processing A PerkinElmer spectrometer equipped with MIR TGS detector was used for recording the spectra (Spectrum 100 Instrument, PerkinElmer Inc., Norwalk, CT, USA). FTIR spectra of the samples were recorded between 4000 and 450 cm^{-1}. Interferograms were taken for 20 scans at 4 cm^{-1} resolution and then averaged. The background spectrum was automatically subtracted from the spectra of the samples. All data manipulations were carried out in Spectrum 100 software (PerkinElmer). From each sample, at least three different scans, which gave identical spectra, were performed. These replicates (n=5 for both the sensitive and resistant cells) were averaged, and the averaged spectra for each sample were then used for further data manipulation and statistical analysis.

For the visual demonstration of the spectral data, the spectra were interactively baselined from two arbitrarily selected points. Then the spectra were normalized in specific regions for visual comparison of ponatinib-treated imatinib-sensitive and imatinib-resistant samples [19].

Since water was removed from the samples in the sample preparation steps using lyophilization procedures, therefore water's contribution to the amide bands was negligible in this study.

Statistical analysis The differences between the ponatinib-treated imatinib-sensitive and imatinib-resistant groups were compared using the Mann–Whitney *U* test with the Matlab R2011a program. The statistical results are expressed as means±standard deviation. $P<0.05$ was considered statistically significant.

Results

Ponatinib showed dose-dependent cytotoxicity on K562 and K562/IMA-3 cells To assess antiproliferative effects of ponatinib on K562 and K562/IMA-3 cells, the cells were treated with increasing concentrations of ponatinib (0.5 to 100 nM) for 72 h and MTT cell proliferation assay was conducted. The results showed that there were dose-dependent decreases in cell proliferation in response to ponatinib as compared to untreated controls. IC_{50} values were calculated from cell proliferation plots and were found to be 1.72 and 28.5 nM, in K562 and K562/IMA-3 cells, respectively (Fig. 1).

Ponatinib-induced loss of MMP in K562 and K562/IMA-3 cells in a dose-dependent manner In order to examine the

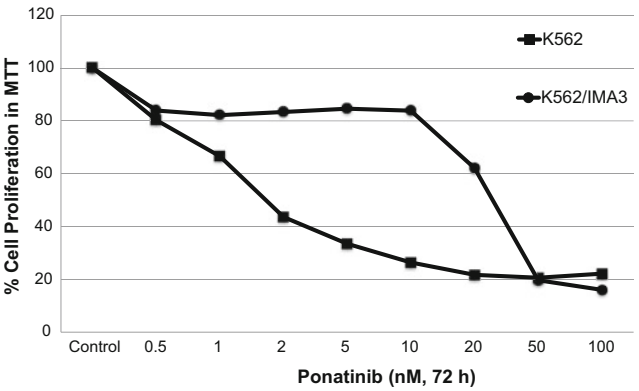

Fig. 1 Cytotoxic effects of ponatinib in K562 and K562/IMA-3 cells treated with increasing concentrations of ponatinib (0.5–100 nM) for 72 h at 37 °C. $P<0.05$ was considered to be significant. The *error bars* represent the standard deviations, and when not seen, they are smaller than the thickness of the lines on the graphs

apoptotic effects of ponatinib on K562 and K562/IMA-3 cells, we treated the cells with increasing concentrations of ponatinib (10 to 100 nM) for 72 h and analyzed the changes in loss of MMP. The results showed that the increasing concentrations of ponatinib significantly increased the MMP. There were 1.3- to 3.6-fold and 1- to 6.6-fold increases in loss of MMP in K562 and K562/IMA-3 cells in response to ponatinib, respectively, as compared to untreated controls (Fig. 2).

Ponatinib treatment increased caspase-3 enzyme activity in K562 and K562/IMA-3 cells in a dose-dependent manner K562 and K562/IMA-3 cells were treated with increasing concentrations of ponatinib (10 to 100 nM) for 72 h, and changes in caspase-3 enzyme activity were examined. The results demonstrated that increasing concentrations (10 to 100 nM) of ponatinib increased caspase-3 enzyme activity from 1.8- to 2.4-fold and from 1- to 1.5-fold in K562 and K562/IMA-3 cells, respectively, as compared to untreated controls (Fig. 3).

Ponatinib treatment increased apoptotic cell population of K562 and K562/IMA-3 cells Apoptotic effects of ponatinib were confirmed by examining the apoptotic cell population with an annexin-V FITC assay via flow cytometer. The results showed that the increasing concentrations of ponatinib significantly increased the apoptotic cell populations. Apoptotic cell population increased from approximately 2- to 8.5-fold in K562 cells in response to (10 to 100 nM) ponatinib while there were 7.8- and 9.7-fold increases in K562/IMA-3 cells exposed to 50 and 100 nM ponatinib, respectively (Figs. 4 and 5).

The effects of ponatinib on cell cycle progression of K562 and K562/IMA-3 cells Cytostatic effects of ponatinib on K562 and K562/IMA-3 cells were analyzed via flow cytometer. Cell cycle analyses revealed that ponatinib treatment resulted in cell cycle arrest at G1 phase on K562 and K562/IMA-3 cells (Fig. 6a, b).

The effects of ponatinib on macromolecules in K562 and K562/IMA-3 cells We previously reported our FTIR spectroscopic comparison of imatinib-sensitive and imatinib-resistant K562 cells [20]. However, due to the changes induced by the resistance formation, the response of the drug-sensitive and drug-resistant cells to a second drug was not studied in terms of FTIR spectroscopic means. Therefore, in this study, the structural–metabolic changes induced by ponatinib as the

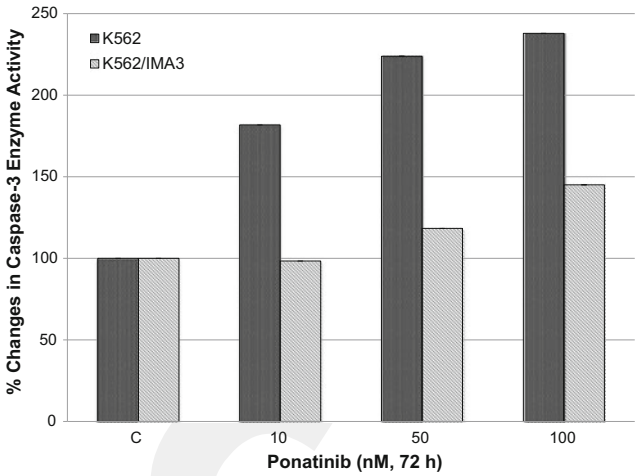

Fig. 3 Effects of ponatinib on changes in caspase-3 enzyme activity in K562 and K562/IMA-3 cells treated with increasing concentrations of ponatinib (10–100 nM) for 72 h at 37 °C. $P<0.05$ was considered to be significant. The *error bars* represent the standard deviations, and when not seen, they are smaller than the thickness of the lines on the graphs

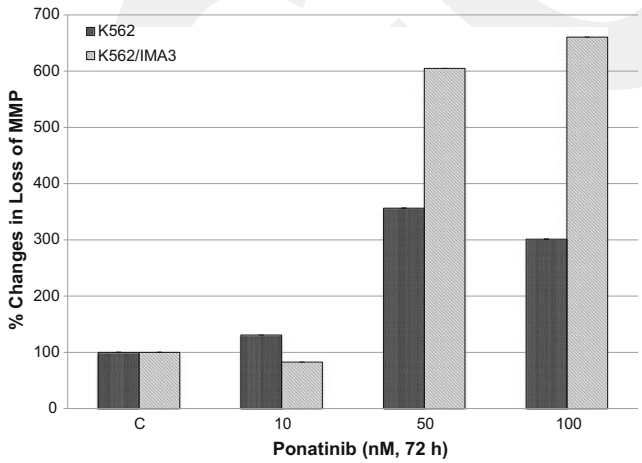

Fig. 2 Effects of ponatinib on changes in MMP in K562 and K562/IMA-3 cells treated with increasing concentrations of ponatinib (10–100 nM) for 72 h at 37 °C. $P<0.05$ was considered to be significant. The *error bars* represent the standard deviations, and when not seen, they are smaller than the thickness of the lines on the graphs

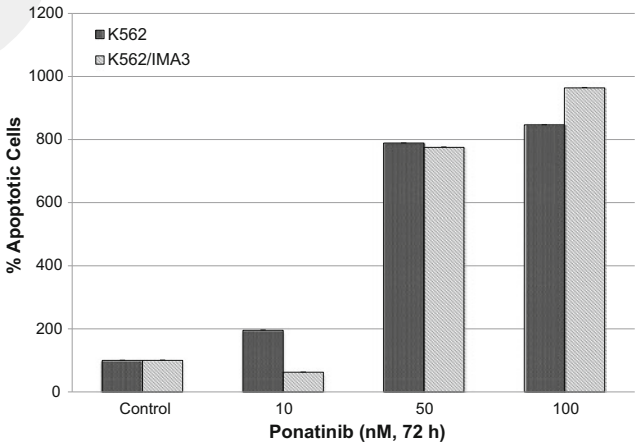

Fig. 4 Effects of ponatinib on apoptotic cell populations in K562 and K562/IMA-3 cells treated with increasing concentrations of ponatinib (10–100 nM) for 72 h at 37 °C. $P<0.05$ was considered to be significant. The *error bars* represent the standard deviations, and when not seen, they are smaller than the thickness of the lines on the graphs

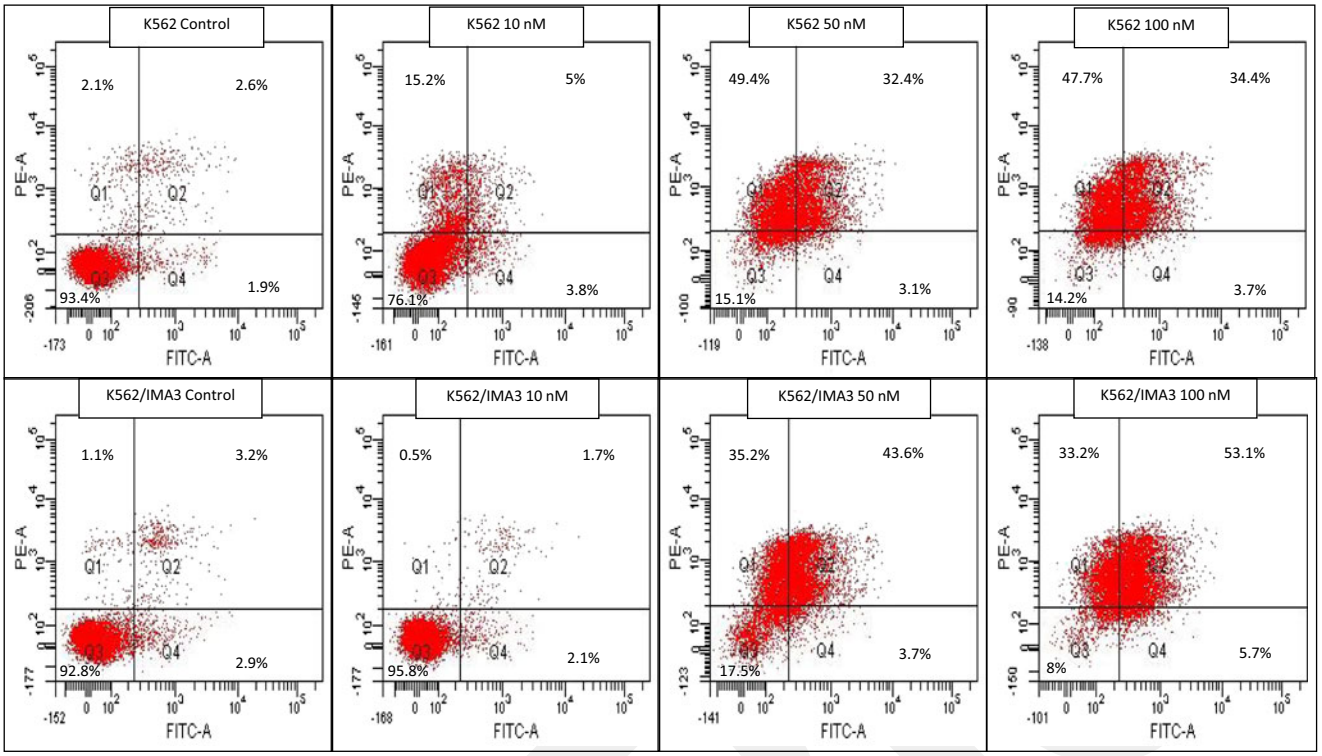

Fig. 5 Quadrant analysis of effects of ponatinib on apoptotic cell populations in K562 and K562/IMA-3 cells treated with increasing concentrations of ponatinib (10–100 nM) for 72 h at 37 °C

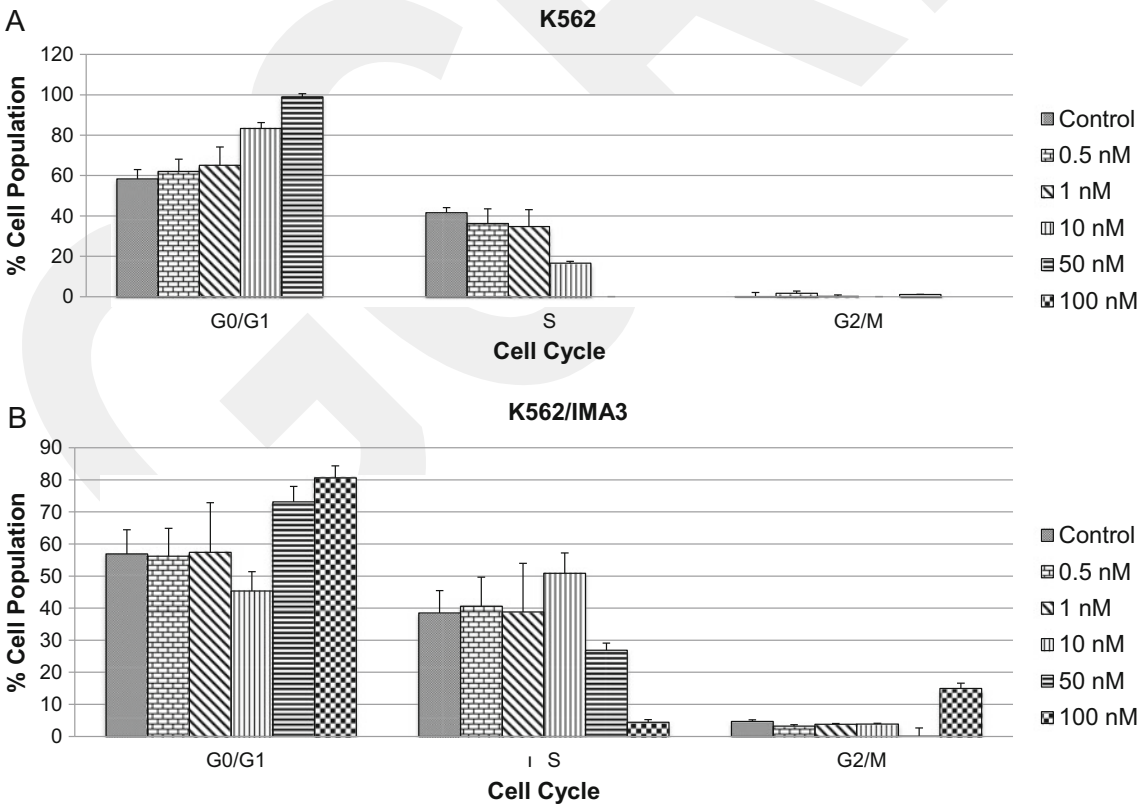

Fig. 6 Effects of ponatinib on cell cycle in K562 (**a**) and K562/IMA-3 (**b**) cells treated with increasing concentrations of ponatinib (0.5–100 nM) for 72 h at 37 °C. $P<0.05$ was considered to be significant. The *error bars* represent the standard deviations, and when not seen, they are smaller than the thickness of the lines on the graphs

second drug on imatinib-sensitive and imatinib-resistant K562 cells were compared using FTIR.

In Fig. 7, the average FTIR spectra of control K562 cells in the 3840–940 cm^{-1} spectral regions were shown. Assignments of the major bands in Fig. 7 are presented in Table 1. The spectra were analyzed for the following regions: 2800–3700 cm^{-1} for the analysis of proteins and lipids, and 1590–1774 cm^{-1} for the analysis of proteins and lipids, 944–1352 cm^{-1} for the analysis of the fingerprint region. In the figures below, all the spectra presented were normalized with respect to specific selected bands and were used only for illustrative purposes. The measurement of the spectral parameters was considered separately for both control and treated groups of the imatinib-sensitive and imatinib-resistant K562 cells.

2800–3700 cm^{-1} region The average FTIR spectra of the sensitive and K562/IMA-3 cells in the 2800–3700 cm^{-1} spectral region are shown in Fig. 8a. Amide A and amide B bands are found in this spectral region. They both have contributions from mainly the N–H stretching of proteins with a small contribution from the O–H stretching of polysaccharides and intermolecular H bonding and contributions from C–N and N–H stretching of proteins, respectively [21].

Ponatinib treatment induced remarkable changes in the bandwidth, intensity, and frequency value of the FTIR bands in this region as seen from Fig. 8 on the both imatinib-sensitive and imatinib-resistant K562 cells. Comparisons of the band intensities of some infrared bands of imatinib-sensitive and imatinib-resistant K562 cells are shown in Fig. 9. In Fig. 8a, the imatinib-sensitive cells were not found to change too much in the amide A band which is located around 3300 cm^{-1} and the amide B band which is located around 3060 cm^{-1}. However, there was a considerable decrease in the intensities of the both bands after ponatinib administration.

When normalized with the intensity of the amide I band, the Amide A/amide I intensity increases 7.72 % for imatinib-sensitive cells but a 9.68 % reduction was observed for imatinib-resistant cells as seen in Fig. 8a, b.

The C–H stretching vibrations of aliphatic compounds are populated between 2996 and 2840 cm^{-1} as shown in Fig. 10. When normalized to the band at 2925 cm^{-1}, the intensity of the CH_3 asymmetric band at 2960 cm^{-1} and CH_3 symmetric stretch band at 2873 cm^{-1} decreased for the imatinib-resistant K562 cells, whereas no significant changes were observed for the imatinib-sensitive K562 cells upon ponatinib administration as seen in Fig. 10a, b.

The intensity ratio of the bands at 2874 and 2852 cm^{-1} decreased by 0.08076 % in the imatinib-sensitive and 2.0886 % for the imatinib-resistant K562 cells ($P<0.0001$). In addition, the intensity ratio of 2852 and 2926 cm^{-1} decreased by 1.1032 % in the imatinib-sensitive and increased by 0.8014 % in the imatinib-resistant K562 cells ($P<0.0001$). The frequency of the CH_3 asymmetric stretch band around 2959 cm^{-1} band shifted from 2960.1417±0.5045 to 2959.6036±0.0914 cm^{-1} in the imatinib-sensitive K562 cells. Similarly, the same band downshifted from 2959.7196±0.1192 to 2959.4966±0.1456 cm^{-1} in the imatinib-resistant K562 cells ($P<0.005$).

1590–1774 cm^{-1} region The average FTIR spectra of the imatinib-sensitive and imatinib-resistant K562 cells upon ponatinib introduction in the 1774–1590 cm^{-1} spectral region is shown in Fig. 11a, b. The band centered at 1740 cm^{-1} is mainly assigned to the C=O ester stretching vibration of triglycerides and cholesterol esters [9, 22, 23]. As seen in the figure, the intensity of the C=O ester stretching vibration did not show significant changes for the imatinib-resistant K562 cell, but for the imatinib-sensitive K562 cells, 3.7462 % decrease was observed. The frequency of the band shows significant changes in the imatinib-resistant K562 cells indicating

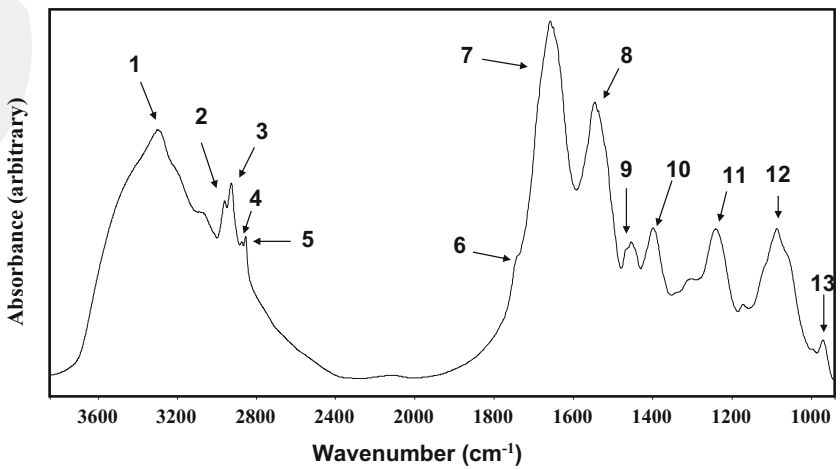

Fig. 7 The general FTIR spectrum of K562 cells in the 3340–940 cm^{-1} region

Table 1 The general FTIR band assignments of K562 cells

Band number	Wavenumbers (cm^{-1})	Definition of the spectral assignment
1	3294	Amide A: mainly N–H stretching of proteins with the little contribution from O–H stretching of polysaccharides and intermolecular bonding
2	2960	CH_3 asymmetric stretch: mainly lipids, with the little contribution from proteins and carbohydrates
3	2925	CH_2 asymmetric stretch: mainly lipids and the little contribution from proteins and carbohydrates
4	2873	CH_3 symmetric stretch: mainly proteins, with the little contribution from lipids and carbohydrates
5	2854	CH_2 symmetric stretch: mainly lipids, with the little contribution from proteins, nucleic acids, and carbohydrates
6	1743	Ester C=O stretch: triglycerides and cholesterol esters
7	1655	Amide I: proteins, mainly C=O stretch
8	1545	Amide II: proteins, mainly N–H bend and C–N stretch
9	1453	CH_2 bending: mainly lipids, with the little contribution from proteins, CH_3 asymmetric bending: methyl groups of proteins
10	1399	COO– symmetric stretch: mainly lipids with the little contribution from proteins; CH_3 symmetric bending: methyl groups of proteins
11	1240	PO_2^- asymmetric stretch: mainly nucleic acids with the little contribution from phospholipids
12	1086	PO_2^- symmetric stretch: nucleic acids and phospholipids; C–O stretch: glycogen
13	970	C–N+–C stretch: nucleic acids

significant changes in the composition of the neutral lipids found in the imatinib-resistant K562 cells. The band at 1659 cm^{-1} is amide I of proteins. Its shape is indicative of protein secondary structures. Since the shapes of the bands did not show significant changes upon ponatinib introduction, it can be said that ponatinib did not introduce significantly different changes in the both imatinib-sensitive and imatinib-resistant K562 cells. A similar behavior was observed when the Amide I/amide II ratios were considered. This ratio increased by only 0.6429 % for the imatinib-sensitive K562 cells and increased by 0.8851 % for the imatinib-resistant K562 cells upon ponatinib administration.

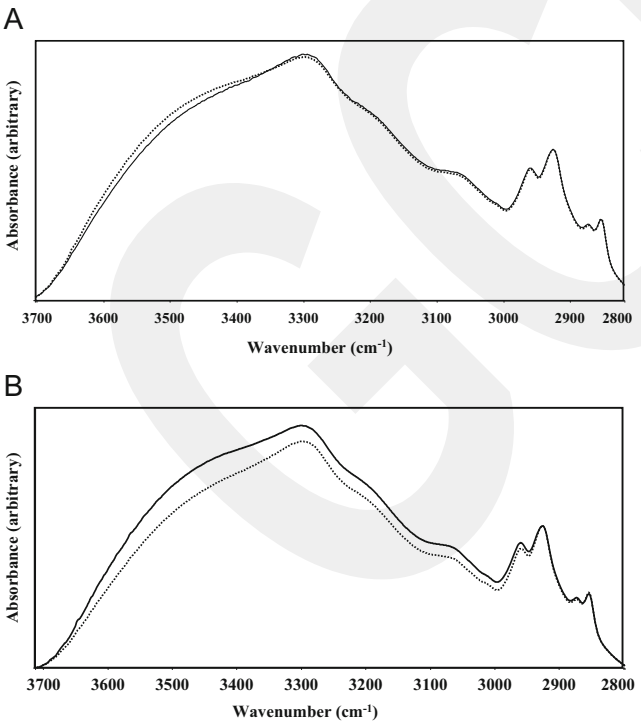

Fig. 8 The FTIR spectra of the ponatinib-treated (*dotted line*) and control (*continuous line*) imatinib-sensitive (**a**) and imatinib-resistant (**b**) K562 cells between 3700 and 2800 cm^{-1} (the spectra were normalized with respect to the CH_2 asymmetric stretch band, which is observed at 2925 cm^{-1})

944–1352 cm^{-1} (fingerprint) region The FTIR spectra in the 944–1352 cm^{-1} region is named fingerprint region. The bands in this spectral region showed significant changes upon ponatinib administration as shown in Fig. 11a, b. The band at 1452 cm^{-1} is attributed to CH_2 bending vibration of lipids [24, 25] as seen in Fig. 11a. The changes in the intensity of the shoulder around 1465 cm^{-1} are more pronounced in the imatinib-resistant K562 cells upon ponatinib introduction. The bands at 1239 and 1086 cm^{-1} are of nucleic acids and attributed to PO_2^- asymmetric and symmetric stretch [26, 27]. The intensity of the band at 1239 cm^{-1} increased significantly in the imatinib-resistant cells. In addition, the changes in the intensities of these bands were seen to be more drastic in the imatinib-resistant cells in Fig. 12b. A shoulder around the band at 1040 cm^{-1} indicates significant changes in the nucleic acids of imatinib-resistant K562 cells. The band at 1155 cm^{-1} is attributed to C–O stretching of glycogen [28]. A notable increase in the intensity of this band was observed in both types of cells but in the imatinib-resistant cells being more pronounced as seen in Fig. 12b. The band at 970 cm^{-1} is assigned to C–N^+–C stretch of nucleic acids [29].

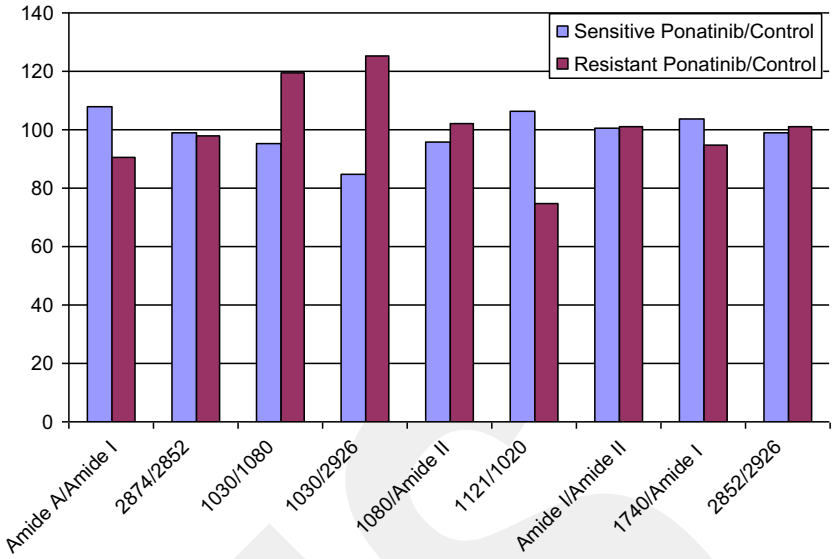

Fig. 9 The intensity ratio of the bands for imatinib-sensitive and imatinib-resistant K562 cells for ponatinib-treated and untreated groups

In the analysis of the bands in this region, the intensity ratio of the 1030 cm^{-1} and 1080 cm^{-1} bands decreased by 4.9416 % in the sensitive K562 cells but increased by 19.6072 % in the resistant K562 cells ($P<0.005$). Similarly, in the same figure, the intensity ratio of 1030 and 2926 cm^{-1} bands decreased by 15.2156 % ($P<0.005$) and increased by 25.4531 % in the resistant cells; 1080 cm^{-1} and amide II bands decreased by 4.46 % in the sensitive cells whereas they increased by 1.9668 % in the resistant cells ($P<0.005$). A decent increase (6.4279 %) in the sensitive cells and a considerable decrease (25.4922 %) in the intensity ratio of the 1121 and 1020 cm^{-1} bands were observed in the imatinib-resistant cells ($P<0.005$).

For a more detailed study in this region, a secondary derivative analysis was carried out. For this purpose, the second derivative of each baseline corrected sample was

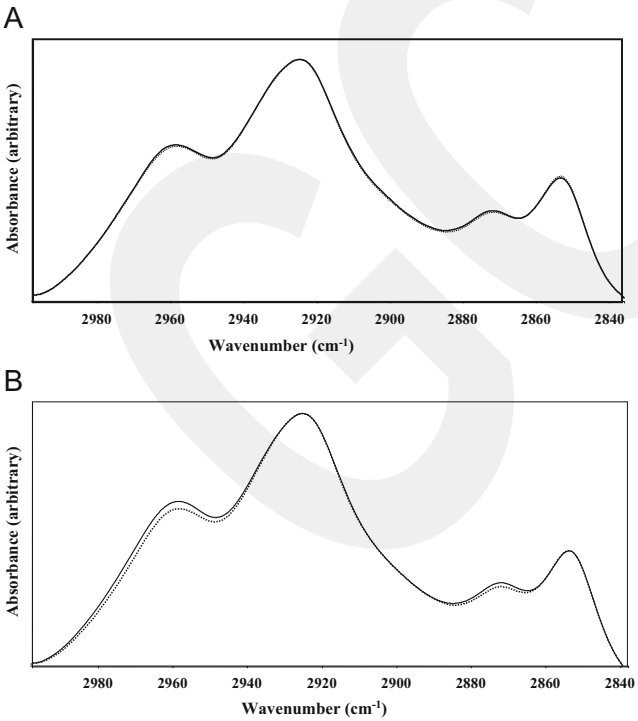

Fig. 10 The FTIR spectra of ponatinib-treated (*dotted line*) and untreated (*solid line*) imatinib-sensitive (**a**) and imatinib-resistant (**b**) K562 cells between 2996 and 2840 cm^{-1} (the spectra were normalized with respect to the amide I band, which is observed at 2925 cm^{-1})

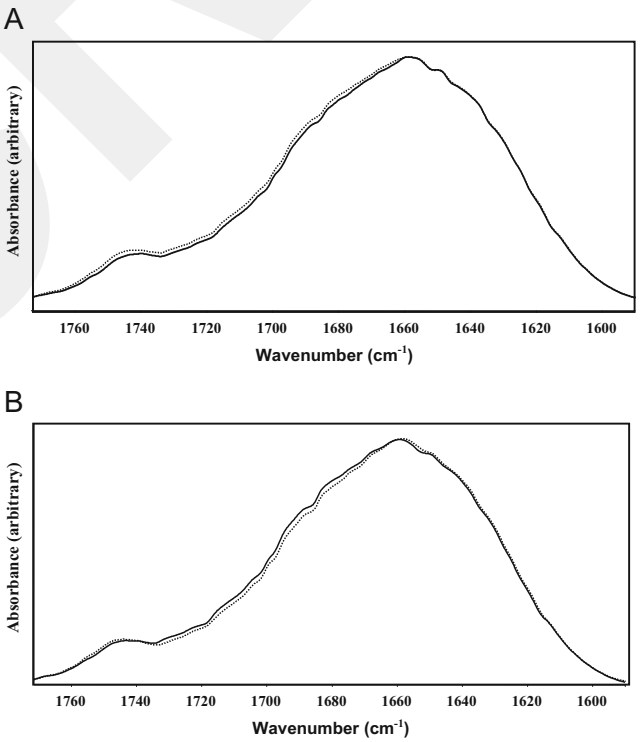

Fig. 11 The FTIR spectra of ponatinib-treated (*dotted line*) and control (*solid line*) imatinib-sensitive (**a**) and imatinib-resistant (**b**) K562 cells between 1774 and 1590 cm^{-1} (the spectra were normalized with respect to the amide I band, which is observed at 1659 cm^{-1})

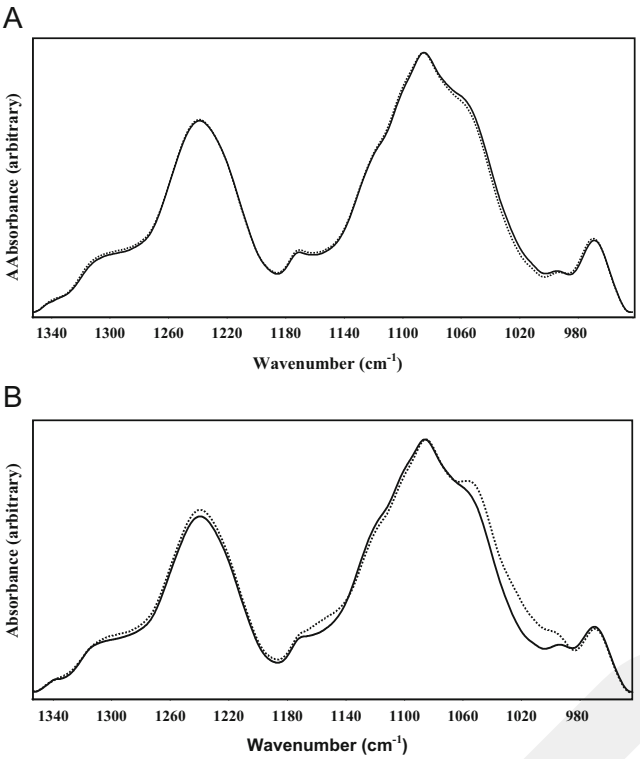

Fig. 12 The FTIR spectra of ponatinib-treated (*dotted line*) and control (*solid line*) imatinib-sensitive (**a**) and imatinib-resistant (**b**) K562 cells between 1352 and 944 cm^{-1} (the spectra were normalized with respect to the amide I band, which is observed at 1080 cm^{-1})

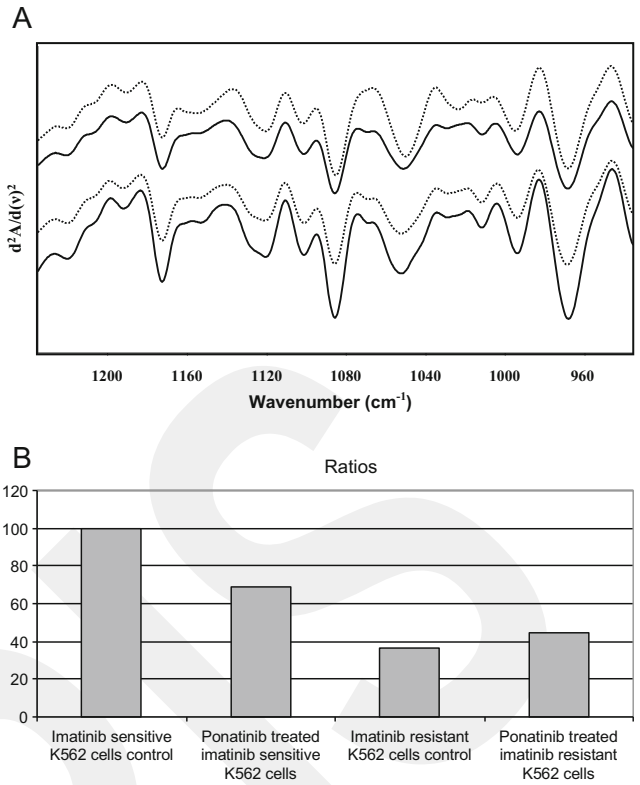

Fig. 13 The average second derivative spectra of imatinib-sensitive and imatinib-resistant (*the uppermost spectra*) K562 cells for ponatinib-treated (*dotted line*) and untreated (*solid line*) groups

taken and their peak minimum was recorded. The average second derivative spectra for the ponatinib-treated and untreated K562 imatinib-sensitive and imatinib-resistant cells are represented in Fig. 13a, b. The intensity ratio of the second derivative spectra for 1069 cm^{-1} (disordering structure) and 1053 cm^{-1} (ordering structure) was studied as the measure of nucleic acid structural order [30]. Our results indicated that as ponatinib was applied, the sensitive cells did not experience a change in their order status; however, the same treatment created a more ordered nucleic acid structure in the resistant cells. In addition, it was clear that resistant cells had more ordered nucleic acid structures when compared with the sensitive counterparts.

FTIR spectroscopic comparison on the lipid profiles of ponatinib treatment The possible changes in the lipid metabolism of K562 cells were tested using the FTIR method on the lipid extracts of the cells. The FTIR spectra of the lipid extracts of the imatinib-sensitive and imatinib-resistant K562 cells indicated several important changes as can be seen in Fig. 14a, b. The assignments of the major peaks in the lipid extract spectra are given in Table 2.

The FTIR spectra of the sensitive and resistant cells were investigated in two different spectral regions. In the first region, the spectra were investigated between 3134 and 2800 cm^{-1} as represented in Fig. 14a, b. In the second part, the region between 1800 and 630 cm^{-1} was investigated as shown in Fig. 15a, b. It is seen in Fig. 16a, b that the cholesterol peak at around 698 cm^{-1} increased with ponatinib treatment in the imatinib-resistant K562 cells much higher than that for imatinib-sensitive K562 cells. In general, it is seen that ponatinib treatment affects imatinib-resistant cells more dramatically than imatinib-sensitive K562 cells. A new band arose as seen in Fig. 15b at 3083, 3061, and 3026 cm^{-1}. The intensity changes in the lipid extracts (Fig. 17) of the sensitive and resistant cells observed upon ponatinib treatment were used to calculate the physical variables as presented in Table 3. In all cases, these variables were observed to increase after ponatinib treatment except for lipids without phosphate for imatinib-resistant K562 cells. In addition, the difference in the changes in the number of acyl chains for both types of cells was again significant. However, there have been significant changes in the amounts of these changes.

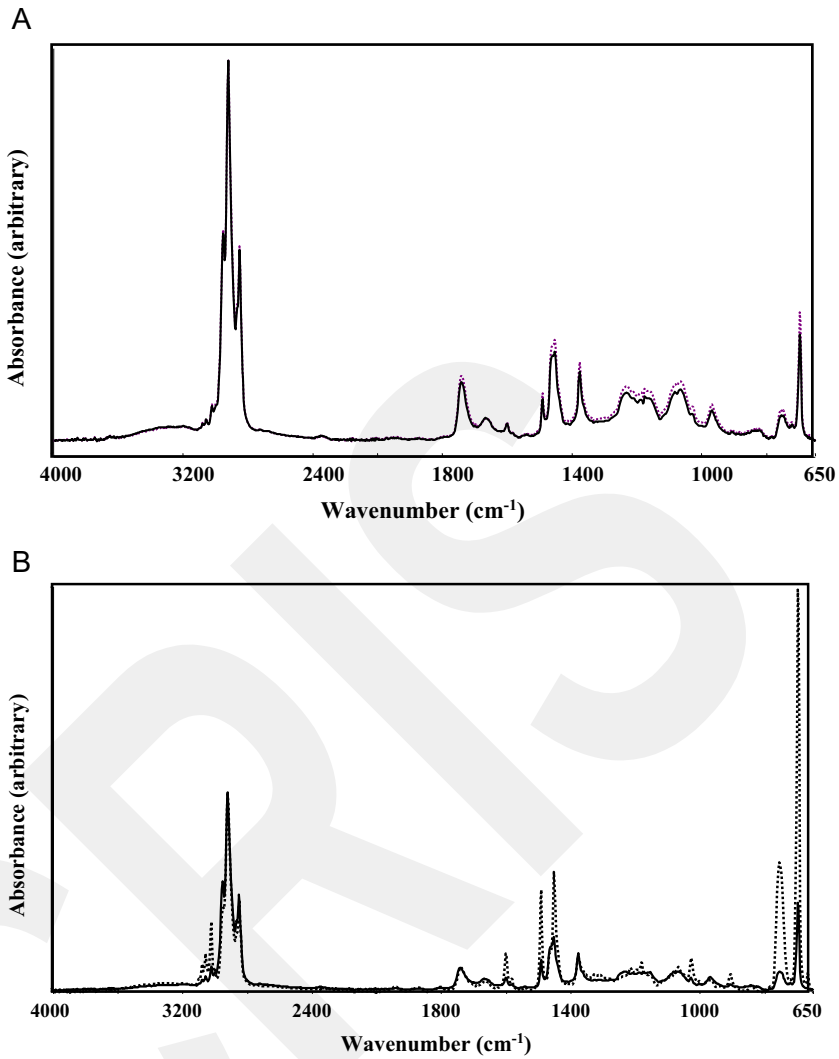

Fig. 14 The general FTIR spectrum of the lipid extracts of ponatinib-treated (*dotted line*) and control (*continuous line*) imatinib-sensitive (**a**) and imatinib-resistant (**b**) K562 cells in the 4000–650 cm^{-1} region

Discussion

Since BCR/ABL oncoprotein exists broadly in CML patients and has constitutive tyrosine kinase activity affecting downstream pathways related to cell proliferation and survival, it has been considered as an open target for therapeutic applications. Therefore, tyrosine kinase inhibitors have been developed for the therapy [31]. Since 2001, imatinib has been used as "gold standard therapy" due to its strong cytotoxic effects on CML cells [32]. Development of resistance against imatinib as well as the second-generation TKIs, nilotinib and dasatinib, is a major obstacle for CML therapy. The most aggressive cause of this resistance is T315I mutation. Imatinib, nilotinib, and dasatinib, which are frontline therapeutics for CML, cannot be effective for CML patients bearing T315I mutation. Ponatinib, one of the third-generation TKIs, is known to be effective in CML patients even bearing T315I mutation because of its capability to bind to BCR/ABL kinase. In a phase I clinical trial, it has been reported that ponatinib treatment of CML patients with T315I mutation results in hematological response in all of the patients, complete cytogenetic response (CCyR) in 75 % of the patients, and also major molecular response (MMR) in 67 % of the patients [33]. A phase II international clinical study, Ponatinib Ph+

Table 2 The band assignments of the lipid extracts of K562 cells

Wavenumbers (cm^{-1})	Definition of the spectral assignment
3002	Olefinic =CH stretching
2960	CH_3 asymmetric stretching
2925	CH_2 asymmetric stretching
2854	CH_2 symmetric stretching
1743	Ester C=O stretching
1542	N–H bending
1216	PO_2^- stretching
698	Cholesterol

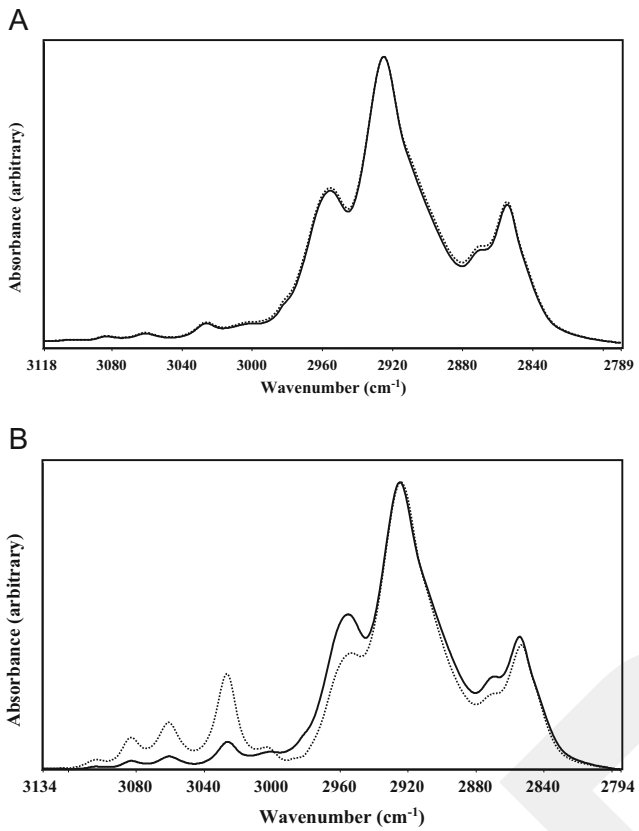

Fig. 15 The FTIR spectra of the lipid extracts of the ponatinib-treated (*dotted line*) and control (*continuous line*) imatinib-sensitive (**a**) and imatinib-resistant (**b**) K562 cells between 3134 and 2800 cm^{-1} (the spectra were normalized with respect to the CH_2 asymmetric stretch band which is located at 2925 cm^{-1})

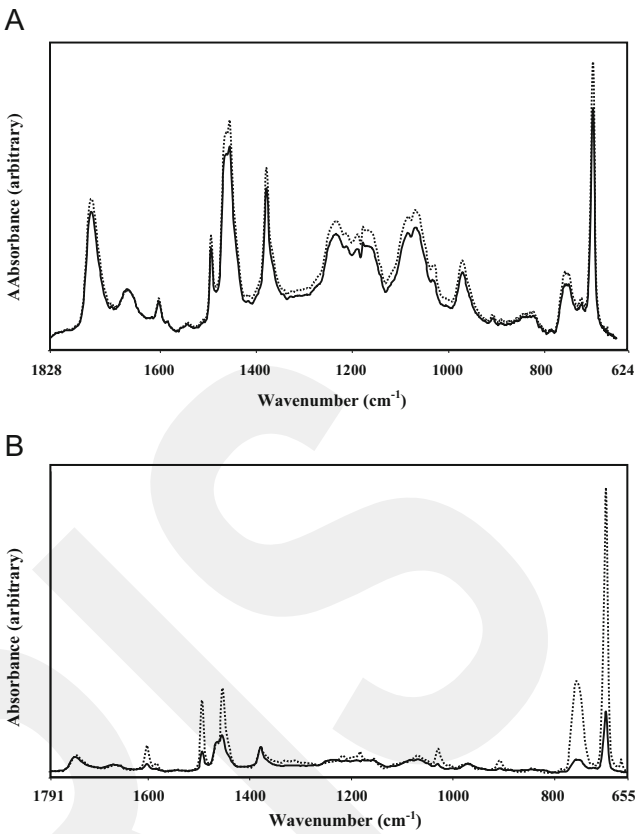

Fig. 16 The FTIR spectra of the lipid extracts of the ponatinib-treated (*dotted line*) and control (*continuous line*) imatinib-sensitive (**a**) and imatinib-resistant (**b**) K562 cells between 1828 and 650 cm^{-1} (the spectra were normalized with respect to the CH_2 asymmetric stretch band which is located at 2925 cm^{-1})

ALL and CML Evaluation (PACE), has reported that CCyR is seen in 46 % of CML patients with T315I mutation [34]. Despite the daily increase of studies on the effects of ponatinib on CML cells, the exact mechanism of action on CML is still unknown.

In this study, we observed cytotoxic, cytostatic, and apoptotic effects of ponatinib on both imatinib-sensitive and imatinib-resistant CML cells. Moreover, we also investigated the effects of ponatinib on changes in the macromolecular structures of imatinib-sensitive and imatinib-resistant CML cells. Our results showed that ponatinib is effective on K562/IMA-3 cells as well as imatinib-sensitive K562 cells, and inhibits cell proliferation (Fig. 1) via triggering apoptosis (Figs. 2, 3, 4, and 5) and cell cycle arrest at G1 phase (Fig. 6). Previously, apoptotic effects of ponatinib were reported in several types of resistant CML cell lines [35], but in this study, we also showed the effects of ponatinib on cell cycle and macromolecular changes in both K562 and K562/IMA-3 cells. Moreover, FTIR results showed that the band around the 3300 cm^{-1} band (amide A) is considered to be due to proteins and polysaccharides. The reduction in the intensity ratios of Amide A to Amide I in the imatinib-resistant cells upon ponatinib treatment can be due to the reduced contribution of glycogen. However, a significant increase was observed in the intensity of the 1155 cm^{-1} band which is mainly assigned to the C–O stretching vibrations in glycogen [36].

Table 3 FTIR band ratios of the imatinib-sensitive and imatinib-resistant K562 cells after ponatinib treatment

	Unsaturation index	Hydrocarbon chain length	PO_2/CH_2	Lipids without phosphate	Number of acyl chains	698 cm/2924 cm
K562 cells	1.0531	1.0041	1.0734	21.9373	23.5497	1.2047
K562/IMA-3 cells	2.5863	1.2344	2.1791	0.7780	1.6955	4.2079

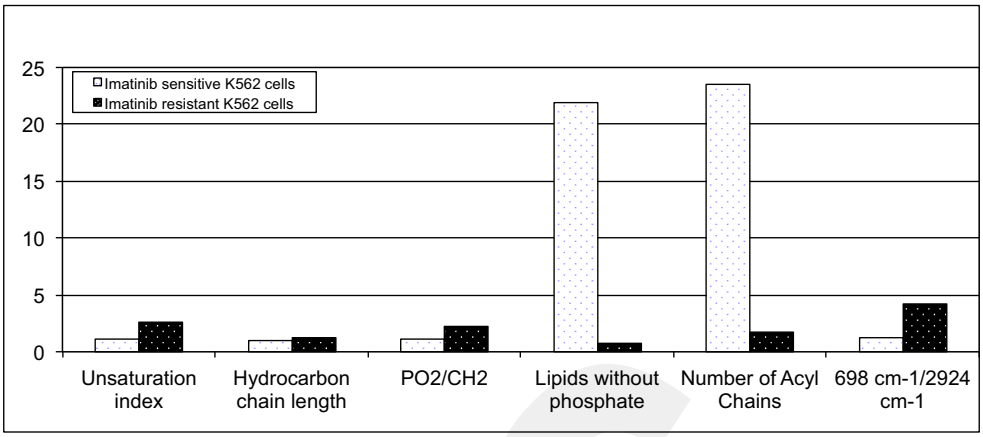

Fig. 17 The intensity ratio of the lipid extract FTIR bands for imatinib-sensitive and imatinib-resistant K562 cells for ponatinib-treated and untreated groups

Cancer cells are known to consume more carbohydrate due to their increased energy expenditure which is known as the Warburg effect [37]. In a similar way, MDR resistance is hypothesized to require more energy for the additional tasks of elimination of toxic compounds and drugs. Therefore, the changes in the level of glycogen in the cancer cells upon ponatinib application should be considered in more detail.

The decrease in CH_3 asymmetric stretching vibration absorption intensity in the imatinib-resistant cells indicates a change in the composition of the acyl chains in lipids as shown in Fig. 2. In addition, the frequency of the CH_3 asymmetric stretch band downshifted in the both imatinib-sensitive and imatinib-resistant K562 cells similarly indicating decreasing freedom of the acyl chain in the center of the bilayer since the CH_3 asymmetric stretching mode is correlated with the order of the deep interior of the membrane [38]. Hence, the order in the lipid plasma membrane interior is increased in the resistant cancer cells [39]. In addition, the intensity of the CH_2 symmetric stretching band decreased in the resistant cells indicating a decreasing proportion of the CH_2 groups in the resistant cells more than that in the sensitive K562 cells. Similarly, the frequency of the bending vibration at around 1453 cm^{-1} upshifted in both imatinib-sensitive and imatinib-resistant K562 cells indicating changes in the lateral packing property of the methylene groups in the membrane lipids [40].

The DNA/protein ratio is estimated by the ratio of 1086 cm^{-1} and amide II bands (41). This ratio 4.35 % decreased for the sensitive but 1.97 % increased for the imatinib-resistant K562 cells indicating a small decrease in the DNA/protein ratio in the sensitive cells.

The glucose/phosphate ratio is given as the intensity ratio of 1030 and 1086 cm^{-1} bands as a reliable measure of the metabolic turnover of the cells [41, 20]. It was found to decrease by 4.94 % in the imatinib-sensitive and increase by 19.61 % in the imatinib-resistant K562 cells. This ratio was found to decrease in malignant transformation when compared with the normal tissues (Gazi et al.). Similarly, the 1030 and 2926 cm^{-1} band ratio was found to decrease by 15.22 for the imatinib-sensitive and increase by 25.46 % in the imatinib-resistant K562 cells indicating decreasing glucose and increasing phospholipid ratios for the sensitive and vice versa for the resistant cells.

The intensity ratio of the 1121 and 1020 cm^{-1} bands was observed to increase for the sensitive (6.43 %) and decrease for the imatinib-resistant cells (25.50 %). This ratio is indicative of the RNA/DNA ratio [20] and was found to increase in the malignant cells when compared with the normal tissues.

The Amide I/Amide II ratio stays at similar levels for both imatinib-sensitive and imatinib-resistant K562 cells upon ponatinib treatment.

The ratio of 1740 cm^{-1}/Amide I bands is indicative of lipid to protein ratio of the analyzed systems [42]. This ratio indicates an increase (3.75 %) in the imatinib-sensitive cells but experiences a decrease in the imatinib-resistant cells (3.04 %) upon ponatinib treatment.

Dovbeshko et al. [30] studied the structural alterations of anticancer drugs such as doxorubicin on the drug-sensitive and resistant cancer cells using surface-enhanced FTIR spectroscopy via the analysis of nucleic acid structure. In their research, they found that upon treatment with doxorubicin, the degree of disorder increased in the doxorubicin-sensitive cancer cells; however, the same parameter was found to decrease in the drug-resistant cancer cells. In this research, we followed their procedure to understand ponatinib-induced changes in the sugar–nucleic acid backbone of the treated K562 cells. The results of the experiments indicated that ponatinib treatment decreases disorder in the imatinib-sensitive K562 cells whereas the disorder in the nucleic acids increased in the resistant K562 cells.

FTIR spectra obtained from the lipid extracts of the both sensitive and resistant cells indicated changes upon ponatinib application. However, the changes with the resistant cells were more drastic when compared with that in the sensitive cells. One of the most important changes was observed in the lipids without phosphate indicating either a decrease in the phosphate-containing lipids or an increase in the fatty acids

or triglycerides and number of acyl chains indicating an increase in the ester-containing lipids. In addition, important changes were observed in the cholesterol amounts. In the resistant cells, the relative ratio of cholesterol when normalization was carried out according to 2926 cm^{-1} band as shown in Figs. 10 and 11. Degree of unsaturation and hydrocarbon chain length increased upon ponatinib treatment in the both sensitive and resistant cells.

Acknowledgments This study was partly supported by TUBITAK project number 107S317 to Y.B. We thank İzmir Institute of Technology, Bioengineering and Biotechnology Application and Research Center for their assistance.

Conflicts of interest None

References

1. Cea M, Cagnetta A, Nencioni A, Gobbi M, Patrone F. New insights into biology of chronic myeloid leukemia: implications in therapy. Curr Cancer Drug Targets. 2013;13:711–23.
2. Pavlovsky C, Kantarjian H, Cortes JE. First-line therapy for chronic myeloid leukemia: past, present, and future. Am J Hematol. 2009;84:287–93.
3. O'Brien S, Radich JP, Abboud CN, Akhtari M, Altman JK, Berman E, et al. Chronic myelogenous leukemia, version 1.2014. J Natl Compr Cancer Netw. 2013;11:1327–40.
4. Kimura S, Ando T, Kojima K. Ever-advancing chronic myeloid leukemia treatment. Int J Clin Oncol. 2014;19:3–9.
5. Weisberg E, Manley PW, Cowan-Jacob SW, Hochhaus A, Griffin JD. Second generation inhibitors of BCR-ABL for the treatment of imatinib-resistant chronic myeloid leukaemia. Nat Rev Cancer. 2007;7:345–56.
6. La Rosee P, Corbin AS, Stoffregen EP, Deininger MW, Druker BJ. Activity of the Bcr-Abl kinase inhibitor PD180970 against clinically relevant Bcr-Abl isoforms that cause resistance to imatinib mesylate (Gleevec, STI571). Cancer Res. 2002;62:7149–53.
7. O'Hare T, Shakespeare WC, Zhu X, Eide CA, Rivera VM, Wang F, et al. AP24534, a pan-BCR-ABL inhibitor for chronic myeloid leukemia, potently inhibits the T315I mutant and overcomes mutation-based resistance. Cancer Cell. 2009;16:401–12.
8. Jain P, Kantarjian H, Cortes J. Chronic myeloid leukemia: overview of new agents and comparative analysis. Curr Treat Options in Oncol. 2013;14:127–43.
9. Dogan A, Ergen K, Budak F, Severcan F. Evaluation of disseminated candidiasis on an experimental animal model: a Fourier transform infrared study. Appl Spectrosc. 2007;61:199–203.
10. Cakmak G, Togan I, Severcan F. 17Beta-estradiol induced compositional, structural and functional changes in rainbow trout liver, revealed by FT-IR spectroscopy: a comparative study with nonylphenol. Aquat Toxicol. 2006;77:53–63.
11. Kneipp J, Lasch P, Baldauf E, et al. Detection of pathological molecular alterations in scrapie-infected hamster brain by Fourier transform infrared (FT-IR) spectroscopy. Biochim Biophys Acta. 2000;1501:189–99.
12. Gaigneaux A, Ruysschaert JM, Goormaghtigh E. Infrared spectroscopy as a tool for discrimination between sensitive and multiresistant K562 cells. Eur J Biochem. 2002;269:1968–73.
13. Le Gal JM, Morjani H, Manfait M. Ultrastructural appraisal of the multidrug resistance in K562 and LR73 cell lines from Fourier transform infrared spectroscopy. Cancer Res. 1993;53:3681–6.
14. Piskin O, Ozcan MA, Ozsan GH, Ates H, Demirkan F, Alacacioglu I, et al. Synergistic effect of imatinib mesylate and fludarabine combination on Philadelphia chromosome-positive chronic myeloid leukemia cell lines. Turk J Haematol. 2007;24:23–7.
15. Gokbulut AA, Apohan E, Baran Y. Resveratrol and quercetin-induced apoptosis of human 232B4 chronic lymphocytic leukemia cells by activation of caspase-3 and cell cycle arrest. Hematology. 2013;18(3):144–50.
16. Baran Y, Bielawski J, Gunduz U, Ogretmen B. Targeting glucosylceramide synthase sensitizes imatinib-resistant chronic myeloid leukemia cells via endogenous ceramide accumulation. J Cancer Res Clin Oncol. 2011;137(10):1535–44.
17. Goktas S, Baran Y, Ural AU, Yazici S, Aydur E, Basal S, et al. Proteasome inhibitor bortezomib increases radiation sensitivity in androgen independent human prostate cancer cells. Urology. 2010;75(4):793–8.
18. Petkovic M, Vocks A, Müller M, Schiller J, Arnhold J. Comparison of different procedures for the lipid extraction from HL-60 cells: a MALDI-TOF mass spectrometric study. Z Naturforsch. 2005;60c:143–51.
19. Ceylan C, Karacicek B. Structural and functional characterization of solution, gel, and aggregated forms of trypsin in organic solvent-assisted and pH-induced phase changes/tripsin çözelti, jel ve agregat formlarının organik çözgen içeren ve pH-tektiklenmiş faz geçişlerinde yapısal ve fonksiyonel incelenmesi. Turk J Biochem. 2015;40:81–7.
20. Baran Y, Ceylan C, Camgoz A. The roles of macromolecules in imatinib resistance of chronic myeloid leukemia cells by Fourier transform infrared spectroscopy. Biomed Pharmacother. 2013;67:221–7.
21. Melin AM, Perromat A, Deleris G. Pharmacologic application of Fourier transform IR spectroscopy: in vivo toxicity of carbon tetrachloride on rat liver. Biopolymers. 2000;57:160–8.
22. Nara M, Okazaki M, Kagi H. Infrared study of human serum very-low-density and low-density lipoproteins. Implication of esterified lipid C O stretching bands for characterizing lipoproteins. Chem Phys Lipids. 2002;117:1–6.
23. Voortman G, Gerrits J, Altavilla M, Henning M, Van BL, Hessels J. Quantitative determination of faecal fatty acids and triglycerides by Fourier transform infrared analysis with a sodium chloride transmission flow cell. Clin Chem Lab Med. 2002;40:795–8.
24. Manoharan R, Baraga JJ, Rava RP, Dasari RR, Fitzmaurice M, Feld MS. Biochemical analysis and mapping of atherosclerotic human artery using FT-IR microspectroscopy. Atherosclerosis. 1993;103:181–93.
25. Jackson M, Ramjiawan B, Hewko M, Mantsch HH. Infrared microscopic functional group mapping and spectral clustering analysis of hypercholesterolemic rabbit liver. Cell Mol Biol. 1998;44:89–98.
26. Wang JJ, Chi CW, Lin SY, Chern YT. Conformational changes in gastric carcinoma cell membrane protein correlated to cell viability after treatment with adamantyl maleimide. Anticancer Res. 1997;17:3473–7.
27. Wong PT, Wong RK, Caputo TA, Godwin TA, Rigas B. Infrared spectroscopy of exfoliated human cervical cells: evidence of extensive structural changes during carcinogenesis. Proc Natl Acad Sci U S A. 1991;88:10988–92.
28. Chiriboga L, Xie P, Vigorita V, Zarou D, Zakim D, Diem M. Infrared spectroscopy of human tissue. II.A comparative study of spectra of biopsies of cervical squamous epithelium and of exfoliated cervical cells. Biospectroscopy. 1998;4:55–9.
29. Ci YX, Gao TY, Feng J, Guo JQ. Fourier transform infrared spectroscopic characterization of human breast tissue: implications for breast cancer diagnosis. Appl Spectrosc. 1999;53:312–5.
30. Dovbeshko GI, Gridina NY, Kruglova EB, Pashchuk OP. FTIR spectroscopy studies of nucleic acid damage. Talanta. 2000;53:233–46.

31. Pavlovsky C, Kantarjian H, Cortes JE. First-line therapy for chronic myeloid leukemia: past, present, and future. Am J Hematol. 2009;84:287–93.
32. Frazer R, Irvine AE, McMullin MF. Chronic myeloid leukaemia in the 21st century. Ulster Med J. 2007;76(1):8–17.
33. Cortes JE, Kantarjian H, Shah NP, Bixby D, Mauro MJ, Flinn I, et al. Ponatinib in refractory Philadelphia chromosome-positive leukemias. N Engl J Med. 2012;367:2075–88.
34. Cortes JE, Kim DW, Pinilla-Ibarz J, Le Coutre PD, Chuah C, Nicolini FE, Paquette R, Apperley JF, DiPersio JF, Khoury HJ, Rea D, Talpaz M, DeAngelo DJ, Abruzzese E, Baccarani M, Mueller MC, Gambacorti-Passerini C, Wong S, Lustgarten S, Turner CD, Rivera VM, Clackson T, Haluska F, Kantarjian HM, The PACE Study Group. Initial findings from the PACE Trial: a pivotal phase 2 study of ponatinib in patients with CML and Ph+ ALL resistant or intolerant to dasatinib or nilotinib, or with the T315I mutation. ASH Meeting 2012; Abstract 163.
35. Cassuto O, Dufies M, Jacquel A, Robert G, Ginet C, Dubois A, et al. All tyrosine kinase inhibitor-resistant chronic myelogenous cells are highly sensitive to ponatinib. Oncotarget. 2012;3:1557–65.
36. Takahashi H, French SW, Wong PT. Alterations in hepatic lipids and proteins by chronic ethanol intake: a high-pressure Fourier transform infrared spectroscopic study on alcoholic liver disease in the rat. Alcohol Clin Exp Res. 1991;15:219–23.
37. Kim HH, Kim T, Kim E, Park JK, Park SJ, Joo H. The mitochondrial Warburg effect: a cancer enigma. Interdisciplinary Bio Central. 2009;1:1–7.
38. Severcan F, Toyran N, Kaptan N, Turan B. Fourier transform infrared study of the effect of diabetes on rat liver and heart tissues in the CH region. Talanta. 2000;53:55–9.
39. Schuldes H, Dolderer JH, Zimmer G, Knobloch J, Bickeboller R, Jonas D, et al. Reversal of multidrug resistance and increase in plasma membrane fluidity in CHO cells with R-verapamil and bile salts. Eur J Cancer. 2001;37:660–7.
40. Tsvetkova NM, Horvath I, Torok Z, Wolkers WF, Balogi Z, Shigapova N, et al. Small heat-shock proteins regulate membrane lipid polymorphism. Proc Natl Acad Sci U S A. 2002;99:13504–9.
41. Colagar A, Chaichi M, Khadjvand T. Fourier transform infrared microspectroscopy as a diagnostic tool for distinguishing between normal and malignant human gastric tissue. J Biosci. 2011;36:669–77.
42. Kochan K, Maslak E, Chlopicki S, Baranska M. FT-IR imaging for quantitative determination of liver fat content in non-alcoholic fatty liver. Analyst. 2015;140(15):4997–5002.